AIMS Mathematics, 8(12): 30287–30312.
DOI: 10.3934/math.20231547
Received: 26 August 2023
Revised: 24 October 2023
Accepted: 03 November 2023
Published: 08 November 2023

http://www.aimspress.com/journal/Math

Research article

Mathematical modeling for anaerobic digestion under the influence of leachate recirculation

Miled El Hajji*

Department of Mathematics, Faculty of Science, University of Jeddah, Jeddah, Saudi Arabia

* **Correspondence:** Email: miled.elhajji@enit.rnu.tn.

Abstract: In this paper, we proposed and studied a simple five-dimensional mathematical model that describes the second and third stages of the anaerobic degradation process under the influence of leachate recirculation. The state variables are the concentration of insoluble substrate, soluble substrate, produced hydrogen, acetogenic bacteria and hydrogenotrophic-methanogenic bacteria. The growth rates of used bacteria will be of general nonlinear form. The stability of the steady states will be studied by reducing the model to a 3D system. According to the operating parameters of the bioreactor described by the added insoluble substrate, soluble substrate and hydrogen input concentrations and the dilution rate, we proved that the model can admit multiple equilibrium points and we gave the necessary and sufficient assumptions for their existence, their uniqueness and their stability. In particular, the uniform persistence of the system was satisfied under some natural assumptions on the growth rates. Then, a question was answered related to the management of renewable resources where the goal of was to propose an optimal strategy of leachate recirculation to reduce the organic matter (either soluble or insoluble) and keep a limitation of the costs of the recirculation operation during the process. The findings of this work were validated by an intensive numerical investigation.

Keywords: chemostat; anaerobic digestion process; leachate recirculation; stability; uniform persistence; optimal strategy
Mathematics Subject Classification: 34D23, 34K13, 34K20, 37B25, 49K40, 92D30

1. Introduction

Methanization is a natural process of transformation of several organic matter into green energy when degraded by specific bacteria without the presence of oxygen [1]. It produces biogas composed mainly of methane while reducing the organic matter. The residue of digestion (or digestate) is stable, deodorized and freed for the most part of pathogenic germs. Thanks to a better understanding of microbiological mechanisms, the first digesters were designed at the end of the 19th century, especially

for the treatment of urban water. This was to remedy the pestilential odors generated by the simple decantation of wastewater practiced at the time. The first known reference concerns the City of EXETER (United Kingdom), which in 1895 recovered the biogas produced for urban lighting. This type of energy production, widely used and known for a long time, presents a promising solution for the production of renewable energy [2]. Indeed, anaerobic digestion is a multistep process in which a consortium of bacteria acts together on organic matter to transform it into biogas (CH_4, CO_2 and H_2).

A large number of leachate recirculation strategies were tested on experimental operated solid-phase digestion systems. Leachate recirculation played a critical role in methane production enhancement since it is a specific factor to facilitate solid waste degradation [3–8].

Several models have been proposed in the literature to model the process anaerobic digestion [9]. The most famous one is the anaerobic digestion model (ADM1) proposed in [10]. The ADM1 model, which became a benchmark, was validated in several applications. ADM1 takes into account the physical, chemical and biological processes. A total of 19 biochemical processes are included, including decay, hydrolysis, acidogenesis, acetogenesis and methanogenesis [10]. Since the ADM1 model is highly parametrized and very complex to study, some numerical studies are validated [11,12]. Several simpler mathematical models describing microbial competition are inspired from ADM1 [13–20] in order to understand this microbial process. However, a few works studied the influence of the leachate recirculation on a bacterial competition [21, 22]. In this article, we proposed a two-tiered model describing a sytrophic relationship under the influence of the leachate recirculation. The considered bacteria involved in the resulting two-tiered model are the acetogenic bacteria and the hydrogenotrophic-methanogenic bacteria. The acetogenic bacteria grows on the soluble substrate to produce hydrogen, which became an inhibitor to its growth. The hydrogenotrophic-methanogenic bacteria used the hydrogen as an essential substrate for growth. This paper is an extension of previous works [23–29] by considering the influence of the leachate recirculation. A detailed analysis using a general nonlinear growth rate is given in [29] in the particular case without the influence of the leachate recirculation. We have then extended the approach presented in [29] by including the influence of the leachate recirculation into the model and characterizing the existence and stability of the four equilibrium points for general growth rates. Moreover, we proposed an optimal strategy for the leachate recirculation to minimize the organic matter in the process while keeping minimum costs.

This paper is organized as the following: In Section 2, we present a five-dimensional system of differential equations modeling a two-tiered bacterial food-web, including the influence of the leachate recirculation. General assumptions on the bacterial growth rates, solubilization rate and the hydrolysis rate are given, then some technical results including the positivity and boundedness of trajectories and the steady states of the system are discussed in Section 3. In Section 4, the five-dimensional system is reduced to a three-dimensional one. The existence and local and global stability of the steady states are discussed with respect to the operating parameters (the dilution rate and the three input concentrations) and the species growth functions. Next, in Section 5, we discuss the uniform persistence for the reduced dynamics and for the main five-dimensional model. In Section 6, we design an optimal strategy to minimize both the organic matter with the cost of leachate recirculation. In Section 7, we discuss some numerical simulations confirming the obtained theoretical findings. Finally, some concluding remarks are summarized in Section 8.

2. Mathematical model

The anaerobic fermentation is a natural phenomenon that transforms organic matter into several products, mainly composed of methane, carbon dioxide and hydrogen (CH_4, CO_2 and H_2), by the concerted action of a close-knit community of bacteria (Figure 1) by catabolizing anaerobically degradable organic matter to the end products [30]. The biological process consists of two methanogenic bacteria that grow inside a chemostat (Figure 2). The acetogenic bacteria grows on the soluble substrate, but is inhibited by the hydrogen that it produces by itself. However, the hydrogenotrophic-methanogenic bacteria grows on the hydrogen produced by the acetogenic bacteria. The model that we propose hereafter is inspired from a previous model proposed in [29] by adding the influence of leachate recirculation as it is applied in [21,22] with generalized growth rates for both species. Let $S_1(t)$, $S_2(t)$, $P(t)$, $X_1(t)$ and $X_2(t)$ stand for the concentrations of insoluble substrate, soluble substrate, hydrogen, acetogenic bacteria and hydrogenotrophic-methanogenic bacteria inside the chemostat at time t.

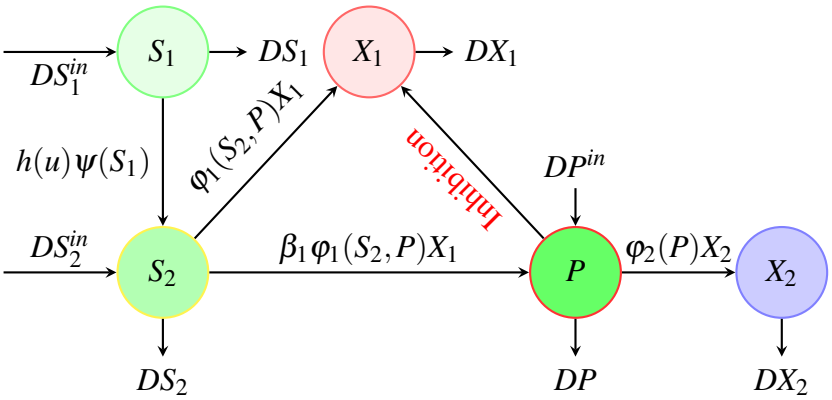

Figure 1. Biological diagram of the interactions of the anaerobic digestion process under the influence of leachate recirculation [29].

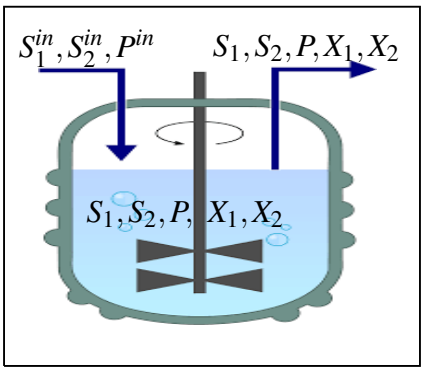

Figure 2. A bioreactor (chemostat) for which the soluble substrate, insoluble substrate, and the hydrogen were added at constant input concentration [31].

By neglecting natural mortality rates with respect to the dilution rate, the proposed mathematical model

takes the following form.

$$\begin{cases} \dot{S}_1 &= D(S_1^{in} - S_1) - h(u)\psi(S_1) \ , \\ \dot{S}_2 &= D(S_2^{in} - S_2) + h(u)\psi(S_1) - \beta_1\varphi_1(S_2,P)X_1 \ , \\ \dot{P} &= D(P^{in} - P) - \beta_2\varphi_2(P)X_2 + \beta_3\varphi_1(S_2,P)X_1 \ , \\ \dot{X}_1 &= \varphi_1(S_2,P)X_1 - DX_1 \ , \\ \dot{X}_2 &= \varphi_2(P)X_2 - DX_2 \ , \end{cases} \tag{2.1}$$

where D is the dilution rate and S_1^{in}, S_2^{in} and P^{in} denote the input concentrations of soluble substrate, insoluble substrate and hydrogen added to the reactor, respectively. The parameters S_1^{in}, S_2^{in}, P^{in}, D, β_1, β_2, β_3 are positive and constant and the functional responses of the species $\varphi_1 : \mathbb{R}_+^2 \to \mathbb{R}_+$ and $\varphi_2 : \mathbb{R}_+ \to \mathbb{R}_+$ are of class C^1. The functions $\psi : \mathbb{R}_+ \to \mathbb{R}_+$ and $h : \mathbb{R}_+ \to \mathbb{R}_+$ are C^1 on $\mathbb{R}_+$.

The meaning of both the parameters and the variables is resumed in Table 1.

Table 1. Parameters and variables significance of model (2.1).

Notation	Description
u	Leachate recirculation rate (that can be a manipulating variable)
$h(\cdot)$	describes the effects of the leachate recirculation on the hydrolytic phenomenon: the solubilization of insoluble substrate depends on the Leachate flow rate
$\psi(\cdot)$	Hydrolysis rate of insoluble substrate into soluble one
$\mu_1(\cdot,\cdot)$	Specific growth rate of acetogenic bacteria.
$\mu_2(\cdot)$	Specific growth rate of hydrogenotrophic-methanogenic bacteria.
S_1^{in}	Insoluble substrate added concentration
S_2^{in}	Soluble substrate added concentration
P^{in}	Hydrogen added concentration
D	Dilution rate
β_1, β_2	Yield coefficients, expressing the conversion rate of the substrate
β_3	Stochiometric coefficients

We introduce some assumptions.

A1. $\varphi_1(S_1^{in} + S_2^{in} - S_1^* + 2(P^{in} - P), P) > D$, $\forall\, P \geq 0$ such that $\varphi_2(P) \leq D$.
A2. $\varphi_1(0,P) = 0$, $\forall\, P \in \mathbb{R}_+$.
A3. $\dfrac{\partial \varphi_1}{\partial S}(S,P) > 0$, $\forall\, (S,P) \in \mathbb{R}_+^2$.
A4. $\dfrac{\partial \varphi_1}{\partial P}(S,P) < 0$, $\forall\, (S,P) \in \mathbb{R}_+^2$.
A5. $\varphi_2(0) = 0$, $\varphi_2(P^{in}) > D$, $\varphi_2'(P) > 0$, $\forall\, P \in \mathbb{R}_+$.
A6. The functions $\psi(\cdot)$ and $h(\cdot)$ are increasing with bounded derivative and $\psi(0) = h(0) = 0$.

The first Hypothesis (A1) reflects the fact that species one can exceed the inhibition of the hydrogen once the concentration of hydrogen is limiting for species two. This assumption is a necessary and sufficient condition from a mathematical point of view for the existence of the coexistence steady state. Hypothesis A2 results from the fact that no growth can take place for acetogenic bacteria without soluble substrate. Hypothesis A3 means that the growth of acetogenic bacteria increases with volatile

fatty acid. Hypothesis A4 reflects that acetogenic bacteria is inhibited by the hydrogen H_2 that it produces by itself. The equality $\varphi_2(0) = 0$ in Hypothesis A5 means that the hydrogen either introduced to the chemostat or produced by the acetogenic bacteria is essential for the methanogenic bacteria growth, and that the growth of methanogenic bacteria increases with hydrogen present in the chemostat. The bacteria relationship is necessary for methanogenic bacteria, however, it is optional for acetogenic bacteria. This kind of relationship is called "syntrophy".

We transform (2.1) by means of the following changes of variables and notations: $s_1 = \dfrac{2\beta_3}{\beta_1}S_1$, $s_1^{in} = \dfrac{2\beta_3}{\beta_1}S_1^{in}$, $s_2 = \dfrac{2\beta_3}{\beta_1}S_2$, $s_2^{in} = \dfrac{2\beta_3}{\beta_1}S_2^{in}$, $p = P$, $p^{in} = P^{in}$, $x_1 = \beta_3 X_1$, $x_2 = \beta_2 X_2$, $g(s_1) = \dfrac{2\beta_3\psi(S_1)}{\beta_1}$, $\mu_1(s_2,p) = \varphi_1(S_2,P)$ and $\mu_2(p) = \varphi_2(P)$. The equations thus obtained are

$$\begin{cases} \dot{s_1} &= D(s_1^{in} - s_1) - h(u)g(s_1)\ , \\ \dot{s_2} &= D(s_2^{in} - s_2) + h(u)g(s_1) - 2\mu_1(s_2,p)x_1\ , \\ \dot{p} &= D(p^{in} - p) - \mu_2(p)x_2 + \mu_1(s_2,p)x_1\ , \\ \dot{x_1} &= \mu_1(s_2,p)x_1 - Dx_1\ , \\ \dot{x_2} &= \mu_2(p)x_2 - Dx_2\ , \end{cases} \tag{2.2}$$

where $s_1^{in} > 0$, $s_2^{in} > 0$, $p^{in} > 0$, $D > 0$. $\mu_1 : \mathbb{R}_+^2 \to \mathbb{R}_+$, $\mu_2 : \mathbb{R}_+ \to \mathbb{R}_+$, $g : \mathbb{R}_+ \to \mathbb{R}_+$ and $h : \mathbb{R}_+ \to \mathbb{R}_+$ are functions of class C^1. Assumptions *A1* to *A5* become:

H1. $\mu_1(s_1^{in} + s_2^{in} - s_1^* + 2(p^{in} - p), p) > D$, $\forall\ p \geq 0$ such that $\mu_2(p) \leq D$.
H2. $\mu_1(0,p) = 0$, $\forall\ p \in \mathbb{R}_+$.
H3. $\dfrac{\partial \mu_1}{\partial s}(s,p) > 0$, $\forall\ (s,p) \in \mathbb{R}_+^2$.
H4. $\dfrac{\partial \mu_1}{\partial p}(s,p) < 0$, $\forall\ (s,p) \in \mathbb{R}_+^2$.
H5. $\mu_2(0) = 0$, $\mu_2(p^{in}) > D$, $\mu_2'(p) > 0$, $\forall\ p \in \mathbb{R}_+$.
H6. The functions $g(\cdot)$ and $h(\cdot)$ are increasing with bounded derivative where $\psi(0) = h(0) = 0$.

Remark 1. *Typical examples of growth and conversion rates can be given by Monod functions (or also Holling's functions type II).*

$$\mu_1(s,p) = \frac{\bar{\mu}_1 s}{(k_s + s)(k_p + p)}, \mu_2(p) = \frac{\bar{\mu}_2 p}{k_2 + p}, g(s) = \frac{\bar{g}s}{k_3 + s}, h(u) = \frac{\bar{h}u}{k_4 + u}$$

where k_s, k_p, k_2, k_3 and k_4 are Monod constants. $\bar{\mu}_1$, $\bar{\mu}_2$, $\bar{g}$ and $\bar{h}$ are positive constants.

3. Preliminary results

In this section, we will give some technical results, an attractive set and the steady states of system (2.2).

Lemma 1. *If the function $\mu_2 : \mathbb{R}_+ \to \mathbb{R}_+$ satisfies hypothesis H5, then $\exists!\ p^* \in (0, p^{in})$ satisfying*

$$\mu_2(p^*) = D\ . \tag{3.1}$$

Proof. It is evident since $\mu_2(0)=0$, $\mu_2(s_1^{in}+s_2^{in}+p^{in})>D$ and μ_2 is a continuous increasing function. □

Lemma 2. *If a function $g:\mathbb{R}_+\to\mathbb{R}_+$ satisfies Assumption H6, then there exists a unique value $s_1^*\in(0,s_1^{in})$ such that*

$$h(u)g(s_1^*)=D(s_1^{in}-s_1^*)\ . \tag{3.2}$$

Proof. Let $\gamma(s)=D(s_1^{in}-s)-h(u)g(s)$, then $\gamma'(s)=-D-h(u)g'(s)<0$, $\gamma(0)=Ds_1^{in}>0$, $\gamma(s_1^{in})=-h(u)g(s_1^{in})<0$ and γ is a continuous and increasing function. Therefore, there exists a unique value $s_1^*\in(0,s_1^{in})$ satisfying (3.2). □

Remark 2. *Since system (2.2) satisfies Assumptions H2 to H6, then by Lemma 1, the Assumption H1 is equivalent to $\mu_1(s_1^{in}+s_2^{in}+p^{in}-2p^*,p^*)>D$.*

Lemma 3. *Under Assumptions H1 to H6, $\exists\ \bar{p}\in\left(0,p^{in}+\dfrac{s_2^{in}+s_1^{in}-s_1^*}{2}\right)$ satisfying*

$$\mu_1\left(s_2^{in}+s_1^{in}-s_1^*+2(p^{in}-\bar{p}),\bar{p}\right)=D\ . \tag{3.3}$$

Proof. It is evident since $\mu_1(0,p^{in}+\dfrac{s_2^{in}+s_1^{in}-s_1^*}{2})=0$, $\mu_1(s_2^{in}+s_1^{in}-s_1^*+2p^{in},0)>D$ and $p\to\mu_1(s_2^{in}+s_1^{in}-s_1^*+2(p^{in}-p),p)$ is a continuous and decreasing function. □

System (2.2) is defined on the nonnegative cone, satisfying classical properties [32] given hereafter.

Proposition 1. *1) Trajectories of model (2.2) are defined, nonnegative and bounded.*

2) $\Sigma=\left\{(s_1,s_2,p,x_1,x_2)\in\mathbb{R}_+^5\mid s_1+s_2+p+x_1+x_2=s_1^{in}+s_2^{in}+p^{in},\ s_1+s_2+2x_1=s_1^{in}+s_2^{in}\right\}$ is a positively invariant attractor set of trajectories of the dynamics (2.2).

Proof.

1) The invariance of $\mathbb{R}_+^5$ is confirmed as follows: $s_1(t)=0\Rightarrow\dot{s}_1(t)=Ds_1^{in}>0$, $s_2(t)=0\Rightarrow\dot{s}_2(t)=Ds_2^{in}+h(u)g(s_1)>0$, $x_1(t)=0\Rightarrow\dot{x}_1(t)=0$, $p(t)=0\Rightarrow\dot{p}(t)=Dp^{in}+\mu_1(s_2,0)x_1>0$, and $x_2(t)=0\Rightarrow\dot{x}_2(t)=0$.

Consider the variables $z(t)=s_1(t)+s_2(t)+p(t)+x_1(t)+x_2(t)-s_1^{in}-s_2^{in}-p^{in}$ and $\zeta(t)=s_1(t)+s_2(t)+2x_1(t)-s_1^{in}-s_2^{in}$.

By adding all equations of dynamics (2.2), we obtain

$$\dot{z}(t)=-Dz(t)\ , \tag{3.4}$$

and, therefore, we deduce that

$$s_1(t)+s_2(t)+p(t)+x_1(t)+x_2(t)=s_1^{in}+s_2^{in}+p^{in}+z(0)e^{-Dt} \tag{3.5}$$

with $z(0)=s_1(0)+s_2(0)+p(0)+x_1(0)+x_2(0)-s_1^{in}-s_2^{in}-p^{in}$. Similarly,

$$\dot{\zeta}(t)=-D\zeta(t)\ , \tag{3.6}$$

and, therefore, we deduce that

$$s_1(t)+s_2(t)+2x_1(t)=s_1^{in}+s_2^{in}+\zeta(0)e^{-Dt} \tag{3.7}$$

with $\zeta(0)=s_1(0)+s_2(0)+2x_1(0)-s_1^{in}-s_2^{in}$. Since all components of the sum are nonnegative, thus, we deduce the boundedness of the trajectory of dynamics (2.2).

2) It can be obtained from Eqs (3.4) and (3.6). □

Lemma 4. *Consider a solution (s_1,s_2,p,x_1,x_2) of dynamics (2.2). Let the change of variable $\omega_1 = s_1 - s_1^*$ and $\omega_2 = s_1^{in} + s_2^{in} - 2x_1 - s_1 - s_2 = s_1^{in} + s_2^{in} - s_1^* - 2x_1 - \omega_1 - s_2$. Then, $s_1 = \omega_1 + s_1^*$, $s_2 = s_1^{in} + s_2^{in} - s_1^* - 2x_1 - \omega_1 - \omega_2$ and system (2.2) is equivalent to the following subsystems (3.8) and (3.9):*

$$\begin{cases} \dot{\omega}_1 &= -D\omega_1 - h(u)g(\omega_1 + s_1^*) \leq -D\omega_1 \ , \\ \dot{\omega}_2 &= -D\omega_2 \ , \end{cases} \tag{3.8}$$

and

$$\begin{cases} \dot{p} &= D(p^{in} - p) - \mu_2(p)x_2 + \mu_1(s_1^{in} + s_2^{in} - s_1^* - 2x_1 - \omega_1 - \omega_2, p)x_1 \ , \\ \dot{x}_1 &= \mu_1(s_1^{in} + s_2^{in} - s_1^* - 2x_1 - \omega_1 - \omega_2, p)x_1 - Dx_1 \ , \\ \dot{x}_2 &= \mu_2(p)x_2 - Dx_2 \ . \end{cases} \tag{3.9}$$

Proof. The prove of Lemma 4 is evident and it is omitted. □

The next result is consecrated to the steady states of dynamics (2.2).

Theorem 1. *Suppose that dynamics (2.2) satisfies Assumptions H1 to H6, then, dynamics (2.2) admits four, and only four, steady states. There exists $s_2^* \in \mathbb{R}$ such that $0 < s_2^* < s_1^{in} + s_2^{in}$, $f(s_2^*, p^*) = D$, $x_1^* = \dfrac{s_1^{in} + s_2^{in} - s_1^* - s_2^*}{2} > 0$, $x_2^* = \dfrac{s_1^{in} + s_2^{in} - s_1^* - s_2^*}{2} + p^{in} - p^* > 0$ with p^* given by Lemma 1, s_1^* given by Lemma 2 and the steady states of dynamics (2.2) are given by*

$$E^0 = (s_1^*, s_2^{in} + (s_1^{in} - s_1^*), p^{in}, 0, 0) \ , \quad E^1 = (s_1^*, s_2^{in} + (s_1^{in} - s_1^*) + 2(p^{in} - \bar{p}), \bar{p}, \bar{p} - p^{in}, 0) \ ,$$
$$E^2 = (s_1^*, s_2^{in} + (s_1^{in} - s_1^*), p^*, 0, p^{in} - p^*) \text{ and } E^* = (s_1^*, s_2^*, p^*, x_1^*, x_2^*)$$

with $\bar{p}$ defined in (3.3), and moreover, the constants $\bar{p}$, p^* satisfy

$$0 < p^* < p^{in} < \bar{p} < p^{in} + \frac{s_1^{in} + s_2^{in} - s_1^*}{2} \ . \tag{3.10}$$

Proof. Suppose that dynamics (2.2) satisfies Assumptions H1 to H6. Let $E^e = (s_1^e, s_2^e, p^e, x_1^e, x_2^e)$ be a nonnegative steady state of dynamics (2.2), then it satisfies the following system

$$\begin{cases} 0 &= D(s_1^{in} - s_1^e) - h(u)g(s_1^e) \ , \\ 0 &= D(s_2^{in} - s_2^e) + h(u)g(s_1^e) - 2\mu_1(s_2^e, p^e)x_1^e \ , \\ 0 &= D(p^{in} - p^e) - \mu_2(p^e)x_2^e + \mu_1(s_2^e, p^e)x_1^e \ , \\ 0 &= \mu_1(s_2^e, p^e)x_1^e - Dx_1^e \ , \\ 0 &= \mu_2(p_e)x_2^e - Dx_2^e \ , \end{cases} \tag{3.11}$$

which is equivalent to

$$\begin{cases} h(u)g(s_1^e) &= D(s_1^{in} - s_1^e) \ , \\ \mu_1(s_2^e, p^e)x_1^e &= Dx_1^e \ , \\ \mu_2(p_e)x_2^e &= Dx_2^e \ , \\ s_1^e + s_2^e &= s_1^{in} + s_2^{in} + 2x_1^e \ , \\ x_2^e &= x_1^e + p^{in} - p^e \ . \end{cases} \tag{3.12}$$

If $x_1^e = 0$, then we obtain $s_1^e = s_1^*$, $s_2^e = s_1^{in} + s_2^{in} - s_1^*$ and $x_2^e + p^e = p^{in}$. Then, $x_2^e = 0$ and we obtain $E^e = E^0$ or $x_2^e \neq 0$, and then $p^e = p^*$ and $x_2^e = p^{in} - p^*$, then we deduce that $E^e = E^2$.
If $x_1 \neq 0$ and $x_2 = 0$, then we have

$$\begin{cases} h(u)g(s_1^e) &= D(s_1^{in} - s_1^e) \,, \\ \mu_1(s_2^e, p^e) &= D \,, \\ s_1^e + s_2^e &= s_1^{in} + s_2^{in} - 2x_1^e \,, \\ x_1^e &= p^e - p^{in} \,. \end{cases} \tag{3.13}$$

From Lemmas 2 and 3, we obtain $s_1^e = s_1^*$ and $p^e = \bar{p}$ and, therefore, $x_1^e = \bar{p} - p^{in}$. We deduce that $E^e = E^1$.
One case remains where $x_1 \neq 0$ and $x_2 \neq 0$. Therefore, we have

$$\begin{cases} h(u)g(s_1^e) &= D(s_1^{in} - s_1^e) \,, \\ \mu_1(s_2^e, p^e) &= D \,, \\ \mu_2(p^e) &= D \,, \\ s_1^e + s_2^e &= s_1^{in} + s_2^{in} - 2x_1^e \,, \\ x_2^e &= x_1^e + p^{in} - p^e \,. \end{cases} \tag{3.14}$$

From Lemmas 1 and 2, we obtain $p^e = p^*$ and $s_1^e = s_1^*$, and then

$$\begin{cases} \mu_1(s_1^{in} + s_2^{in} + 2p^{in} - s_1^* - 2(x_2^e + p^*), p^*) \;=\; D \,, \\ s_2^e \;=\; s_1^{in} + s_2^{in} - s_1^* - 2x_1^e \;=\; s_1^{in} + s_2^{in} + 2p^{in} - s_1^* - 2(x_2^e + p^*) \,, \\ x_1^e \;=\; x_2^e - p^{in} + p^* \,. \end{cases} \tag{3.15}$$

From Assumption *H1*, we have $\mu_1(s_1^{in} + s_2^{in} + 2p^{in} - s_1^* - 2p^*, p^*) > D$. Since μ_1 is a continuous function and Assumptions H2 and H3 are satisfied, then there exists $x_2^e > 0$ such that $\mu_1(s_1^{in} + s_2^{in} + 2p^{in} - s_1^* - 2(x_2^e + p^*), p^*) = D$ and $s_2^e = s_1^{in} + s_2^{in} - s_1^* - 2x_1^e = s_1^{in} + s_2^{in} + 2p^{in} - s_1^* - 2(x_2^e + p^*) > 0$. Thus, E^e is the positive steady state E^*. □

4. Reduced dynamics and local analysis

In this section, we aim to give an asymptotic analysis of the solutions of system (2.2). Note that dynamics (2.2) is equivalent to the coupled subsystems (3.8) and (3.9), thus, it is sufficient to give the asymptotic analysis for (3.8) and (3.9). One might think that, due to the attractivity of the set Σ, one can straightforwardly deduce from the stability properties of system (3.8) and (3.9) restricted to the invariant set Σ what the stability properties of the coupled system (3.8) and (3.9) are. Observe that (ω_1, ω_2) solution of system (3.8) converges to $(0,0)$, then the system (4.1) is obtained by considering the system (3.8) and (3.9) with $\omega_1 = 0$ and $\omega_2 = 0$. Generally, this is false as highlighted in some references [33,34], but fortunately in the case we consider, it turns out that this is true. We will manage to deduce what is the behavior of the positive solutions of dynamics (3.8) and (3.9) from the asymptotic analysis of the solutions of the following dynamics.

$$\begin{cases} \dot{p} &= \lambda_1(p, x_1, x_2) \,, \\ \dot{x}_1 &= \lambda_2(p, x_1, x_2) \,, \\ \dot{x}_2 &= \lambda_3(p, x_1, x_2) \,, \end{cases} \tag{4.1}$$

with

$$\Lambda(p,x_1,x_2)=\begin{pmatrix}\lambda_1(p,x_1,x_2)\\ \lambda_2(p,x_1,x_2)\\ \lambda_3(p,x_1,x_2)\end{pmatrix}=\begin{pmatrix}D(p^{in}-p)-\mu_2(p)x_2+\mu_1(s_1^{in}+s_2^{in}-s_1^*-2x_1,p)x_1\\ \mu_1(s_1^{in}+s_2^{in}-s_1^*-2x_1,p)x_1-Dx_1\\ \mu_2(p)x_2-Dx_2\end{pmatrix}$$

and with

$$\mathscr{S}=\left\{(p,x_1,x_2)\in(\mathbb{R}_+^*)^3\ :\ 0<x_1<\frac{s_1^{in}+s_2^{in}-s_1^*}{2}\right\}$$

as state space.

From Lemma 4 and Theorem 1, we deduce that the three-dimensional dynamics (4.1) admits $F^0=(p^{in},0,0),$, $F^1=(\bar{p},\bar{p}-p^{in},0)$, $F^2=(p^*,0,p^{in}-p^*)$ and $F^*=(p^*,x_1^*,x_2^*)$ as steady states.

Lemma 5. *Assume that dynamics (2.2) satisfies Assumptions H1 to H6, then F^0, F^1 and F^2 are locally unstable steady states and F^* is a locally exponentially stable steady state for the dynamics (4.1).*

Proof. The Jacobian matrix $J(p,x_1,x_2)\in\mathbb{R}^{3\times3}$ of the function $\Lambda(p,x_1,x_2)$ at a point (p,x_1,x_2) is given by

$$J(p,x_1,x_2)=\begin{bmatrix}-D-\mu_2'(p)x_2+\dfrac{\partial\mu_1}{\partial p}x_1 & \mu_1-2\dfrac{\partial\mu_1}{\partial s_2}x_1 & -\mu_2(p)\\ \dfrac{\partial\mu_1}{\partial p}x_1 & \mu_1-D-2\dfrac{\partial\mu_1}{\partial s_2}x_1 & 0\\ \mu_2'(p)x_2 & 0 & \mu_2(p)-D\end{bmatrix}$$

where the function μ_1 is expressed at $\left(s_1^{in}+s_2^{in}-s_1^*-2x_1,p\right)$. Now, we consider successively the matrices $J(F^0)$, $J(F^1)$, $J(F^2)$ and $J(F^*)$. Since

$$J(F^0)=\begin{bmatrix}-D & \mu_1(s_1^{in}+s_2^{in}-s_1^*,p^{in}) & -\mu_2(p^{in})\\ 0 & \mu_1(s_1^{in}+s_2^{in}-s_1^*,p^{in})-D & 0\\ 0 & 0 & \mu_2(p^{in})-D\end{bmatrix},$$

the eigenvalues of $J(F^0)$ are $\lambda_1=-D<0$, $\lambda_2=\mu_1(s_1^{in}+s_2^{in}-s_1^*,p^{in})-D>0$ by Assumption H1 and $\lambda_3=\mu_2(p^{in})-D>0$ by Assumption H5. Consequently, F^0 is an exponentially unstable steady state of (4.1). The Jacobian at F^1 is simply

$$J(F^1)=\begin{bmatrix}-D+(\bar{p}-p^{in})\dfrac{\partial\mu_1}{\partial p} & D-2(\bar{p}-p^{in})\dfrac{\partial\mu_1}{\partial s_2} & -\mu_2(\bar{p})\\ (\bar{p}-p^{in})\dfrac{\partial\mu_1}{\partial p} & -2(\bar{p}-p^{in})\dfrac{\partial\mu_1}{\partial s_2} & 0\\ 0 & 0 & \mu_2(\bar{p})-D\end{bmatrix},$$

where the function μ_1 is expressed at $(s_2^{in}+(s_1^{in}-s_1^*)+2(p^{in}-\bar{p}),\bar{p})$.
$J(F^1)$ has an eigenvalue $\lambda_1=\mu_2(\bar{p})-D$ and two other eigenvalues of the submatrix

$$S_{F^1}=\begin{bmatrix}-D+(\bar{p}-p^{in})\dfrac{\partial\mu_1}{\partial p} & D-2(\bar{p}-p^{in})\dfrac{\partial\mu_1}{\partial s_2}\\ (\bar{p}-p^{in})\dfrac{\partial\mu_1}{\partial p} & -2(\bar{p}-p^{in})\dfrac{\partial\mu_1}{\partial s_2}\end{bmatrix}.$$

Note that

$$\mathrm{tr}(S_{F^1}) = -D + (\bar{p} - p^{in})\frac{\partial \mu_1}{\partial p} - 2(\bar{p} - p^{in})\frac{\partial \mu_1}{\partial s_2} < 0$$

and

$$\det(S_{F^1}) = 2D(\bar{p} - p^{in})\frac{\partial \mu_1}{\partial s_2} - D(\bar{p} - p^{in})\frac{\partial \mu_1}{\partial p} > 0.$$

Therefore, the matrix S_{F^1} admits two eigenvalues with a negative real part. The inequalities (3.10), the equality $D = \mu_2(p^*)$ and Assumption H5, which ensures that μ_2 is increasing, imply that $\mu_2(\bar{p}) - D > 0$. Consequently, F^1 is an exponentially unstable steady state of (4.1).
The Jacobian at F^2 is simply

$$J(F^2) = \begin{bmatrix} -D - \mu_2'(p^*)(p^{in} - p^*) & \mu_1(s_1^{in} + s_2^{in} - s_1^*, p^*) & -D \\ 0 & \mu_1(s_1^{in} + s_2^{in} - s_1^*, p^*) - D & 0 \\ \mu_2'(p^*)(p^{in} - p^*) & 0 & 0 \end{bmatrix}.$$

The eigenvalues of $J(F^2)$ are $\lambda_1 = -D < 0$, $\lambda_2 = \mu_1(s_1^{in} + s_2^{in} - s_1^*, p^*) - D > 0$ by Assumption H1 and $\lambda_3 = -\mu_2'(p^*)(p^{in} - p^*) < 0$. Consequently, F^2 is an exponentially unstable steady state of (4.1).
The Jacobian at F^* is

$$J(F^*) = \begin{bmatrix} -D - \mu_2'(p^*)x_2^* + \dfrac{\partial \mu_1}{\partial p}x_1^* & D - 2\dfrac{\partial \mu_1}{\partial s_2}x_1^* & -D \\ \dfrac{\partial \mu_1}{\partial p}x_1^* & -2\dfrac{\partial \mu_1}{\partial s_2}x_1^* & 0 \\ \mu_2'(p^*)x_2^* & 0 & 0 \end{bmatrix} \tag{4.2}$$

where the function μ_1 is expressed at $(s_1^{in} + s_2^{in} - s_1^* - 2x_1^*, p^*)$. $J(F^*)$ has an eigenvalue $\lambda_1 = -D < 0$ and two other eigenvalues of the submatrix

$$S_F^* = \begin{bmatrix} \dfrac{\partial \mu_1}{\partial p}(s_1^{in} + s_2^{in} - s_1^* - 2x_1^*, p^*)x_1^* & -2\dfrac{\partial \mu_1}{\partial s_2}(s_1^{in} + s_2^{in} - s_1^* - 2x_1^*, p^*)x_1^* \\ \mu_2'(p^*)x_2^* & 0 \end{bmatrix}. \tag{4.3}$$

Note that

$$\mathrm{tr}(S_F^*) = \frac{\partial \mu_1}{\partial p}(s_1^{in} + s_2^{in} - s_1^* - 2x_1^*, p^*)x_1^* < 0$$

and

$$\det(S_F^*) = 2\mu_2'(p^*)\frac{\partial \mu_1}{\partial s_2}(s_1^{in} + s_2^{in} - s_1^* - 2x_1^*, p^*)x_1^* x_2^* > 0.$$

Therefore, the matrix S_F^* admits two eigenvalues with a negative real part. Thus, the linear approximation of (4.1) at F^* is exponentially stable. □

Theorem 2. *Assume that dynamics (2.2) satisfies Assumptions H1 to H6, then E^0, E^1 and E^2 are locally unstable steady states and E^* is a locally exponentially stable.*

Proof. Assume that Assumptions H1 to H6 hold. It is easy to see that E^0, E^1, E^2, E^* are locally exponentially stable (resp. unstable) steady states of (2.2) if, and only if, F^0, F^1, F^2, F^* are locally exponentially stable (resp. unstable) steady states of (4.1). □

5. Global analysis for the main dynamics

We aim, in this subsection, to investigate the global stability properties of the main dynamics (2.2). Our investigation is divided into two steps. We start by investigating the global stability of the reduced dynamics (4.1). Therefore, we conclude on the global stability properties of the main dynamics (2.2).

5.1. Global analysis for the reduced dynamics

Let start by investigating the global stability of the reduced three-dimensional dynamics (4.1). We need first to prove that $\mathscr{S}$ and $\overline{\mathscr{S}}$ are positively invariant sets for the reduced dynamics (4.1) and that (4.1) admits no periodic orbits on the faces of $\overline{\mathscr{S}}$.

Lemma 6. *Assume that the system (2.2) satisfies Assumptions H1-H6 and consider the reduced dynamics (4.1). The sets $\mathscr{S}$ and $\overline{\mathscr{S}}$ are positively invariant set for the dynamics (4.1).*

Proof. It is evident because we have $\dot{x}_1 = \big(\mu_1(s_1^{in}+s_2^{in}-s_1^*-2x_1,p)-D\big)x_1$.
Next, we consider a trajectory of (4.1) belonging to $\mathscr{S}$. □

5.2. No periodic orbits on the faces for the reduced dynamics

Let us begin by proving that dynamics (4.1) can't have periodic trajectories in one of the faces of the set $\mathscr{S}$.

- Consider a solution of the reduced system (4.1) on the set $\mathscr{S}$ such that $x_2 = 0$,

$$\left\{\begin{array}{rcl} \dot{p} &=& D(p^{in}-p)+\mu_1(s_1^{in}+s_2^{in}-s_1^*-2x_1,p)x_1, \\ \dot{x}_1 &=& \mu_1(s_1^{in}+s_2^{in}-s_1^*-2x_1,p)x_1-Dx_1, \end{array}\right. \tag{5.1}$$

defined on $\mathscr{S}_{px_1}$ given by

$$\mathscr{S}_{px_1} = \left\{(p,x_1)\in\mathbb{R}_+^2 :\ p+x_1\le p^{in}\right\}.$$

The axis $x_1 = 0$ is invariant and the axis $p = 0$ is repulsive since $p = 0$ implies that $\dot{p} > Dp^{in}$. Let us use the change of variables $\kappa_p = \ln(p)$ and $\kappa_1 = \ln(x_1)$ for $p, x_1 > 0$. Therefore, we obtain:

$$\left\{\begin{array}{rcl} \dot{\kappa}_p = & g_p(\kappa_p,\kappa_1) := D(p^{in}e^{-\kappa_p}-1)+\mu_1(s_1^{in}+s_2^{in}-s_1^*-2e^{\kappa_1},e^{\kappa_p})e^{\kappa_1-\kappa_p}, \\ \dot{\kappa}_1 = & g_1(\kappa_p,\kappa_1) := \mu_1(s_1^{in}+s_2^{in}-s_1^*-2e^{\kappa_1},e^{\kappa_p})-D. \end{array}\right. \tag{5.2}$$

Note that

$$\begin{array}{rcl} \dfrac{\partial g_p}{\partial\kappa_p}+\dfrac{\partial g_1}{\partial\kappa_1} &=& -Dp^{in}e^{-\kappa_p}-\mu_1(s_1^{in}+s_2^{in}-s_1^*-2e^{\kappa_1},e^{\kappa_p})e^{\kappa_1-\kappa_p} \\ && +\dfrac{\partial\mu_1(s_1^{in}+s_2^{in}-s_1^*-2e^{\kappa_1},e^{\kappa_p})}{\partial p}e^{\kappa_1}-\dfrac{\partial\mu_1(s_1^{in}+s_2^{in}-s_1^*-2e^{\kappa_1},e^{\kappa_p})}{\partial s_2}e^{\kappa_p} \\ &<& 0. \end{array} \tag{5.3}$$

Let us apply the Dulac's criterion [32] then dynamics (5.2) (and then dynamics (5.1)) has no periodic trajectory. Therefore, dynamics (4.1) has no periodic trajectory in px_1-face ($x_2 = 0$).

- Consider a solution of the reduced system (4.1) on the set $\mathscr{S}$ such that $p = 0$

$$\begin{cases} \dot{x}_1 &= \mu_1(s_1^{in} + s_2^{in} - s_1^* - 2x_1, 0)x_1 - Dx_1, \\ \dot{x}_2 &= -Dx_2, \end{cases} \tag{5.4}$$

defined on $\mathscr{S}_{x_1x_2}$ given by

$$\mathscr{S}_{x_1x_2} = \left\{(x_i, x_2) \in \mathbb{R}^2_+ : \ x_1 + x_2 \leq s_{in}\right\}.$$

The axes $x_1 = 0$ and $x_2 = 0$ are invariant. Let us use the change of variables $\kappa_1 = \ln(x_1)$ and $\kappa_2 = \ln(x_2)$ for $x_1, x_2 > 0$. Therefore, we obtain:

$$\begin{cases} \dot{\kappa}_1 = & g_1(\kappa_1, \kappa_2) := \mu_1(s_1^{in} + s_2^{in} - s_1^* - 2e^{\kappa_1}, 0) - D, \\ \dot{\kappa}_2 = & g_2(\kappa_1, \kappa_2) := -D. \end{cases} \tag{5.5}$$

Note that

$$\frac{\partial g_1}{\partial \kappa_1} + \frac{\partial g_2}{\partial \kappa_2} = -2e^{\kappa_1} \frac{\partial \mu_1(s_1^{in} + s_2^{in} - s_1^* - 2e^{\kappa_1}, 0)}{\partial s_2} < 0. \tag{5.6}$$

Let us apply the Dulac's criterion [32] then dynamics (5.5) (and then dynamics (5.4)) has no periodic trajectory. Therefore, dynamics (4.1) has no periodic trajectory in x_1x_2-face ($p = 0$).

- Consider a solution of the reduced system (4.1) on the set $\mathscr{S}$ such that $x_1 = 0$

$$\begin{cases} \dot{p} &= D(p^{in} - p) - \mu_2(p)x_2, \\ \dot{x}_2 &= \mu_2(p)x_2 - Dx_2, \end{cases} \tag{5.7}$$

defined on $\mathscr{S}_{px_2}$ given by

$$\mathscr{S}_{px_2} = \left\{(p, x_2) \in \mathbb{R}^2_+ : \ p + x_2 \leq p^{in}\right\}.$$

The axis $x_2 = 0$ is invariant and the axis $p = 0$ is repulsive since $p = 0$ implies that $\dot{p} > Dp^{in}$. Let us use the change of variables $\kappa_p = \ln(p)$ and $\kappa_2 = \ln(x_2)$ for $p, x_2 > 0$. Therefore, we obtain:

$$\begin{cases} \dot{\kappa}_p = & g_p(\kappa_p, \kappa_2) := D(p^{in}e^{-\kappa_p} - 1) - \mu_2(e^{\kappa_p})e^{\kappa_2 - \kappa_p}, \\ \dot{\kappa}_2 = & g_2(\kappa_p, \kappa_2) := \mu_2(e^{\kappa_p}) - D. \end{cases} \tag{5.8}$$

Note that

$$\frac{\partial g_p}{\partial \kappa_p} + \frac{\partial g_2}{\partial \kappa_2} = -Dp^{in}e^{-\kappa_p} + (\mu_2(e^{\kappa_p}) - e^{\kappa_p}\mu_2'(e^{\kappa_p}))e^{\kappa_2 - \kappa_p} < 0. \tag{5.9}$$

Let us apply the Dulac's criterion [32] then dynamics (5.8) (and then dynamics (5.7)) has no periodic trajectory. Therefore, dynamics (4.1) has no periodic trajectory in px_2-face ($x_1 = 0$).

5.3. Persistence for the reduced dynamics

Let us demonstrate that p, x_1 and x_2 converge to nonnegative values through the uniform persistence theory that will apply to system (4.1). Since the steady states of (4.1) given by F^0, F^1 and F^2 are the only boundary equilibrium points, which are saddle points, then we can use a similar proof as the one given in [14, 15, 18, 20] using Butler-McGehee Lemma [32] several times.

Theorem 3. *The reduced model (4.1) is persistent.*

Proof. Note that faces px_1 and px_2 of $\mathscr{S}$ are invariant and that the third face x_1x_2 is repulsive since $p = 0$ implies that $\dot{p} > Dp^{in}$. For clarity, we represent in Figure 3 the configuration of the stable and unstable manifolds of the boundary equilibria of system (4.1).

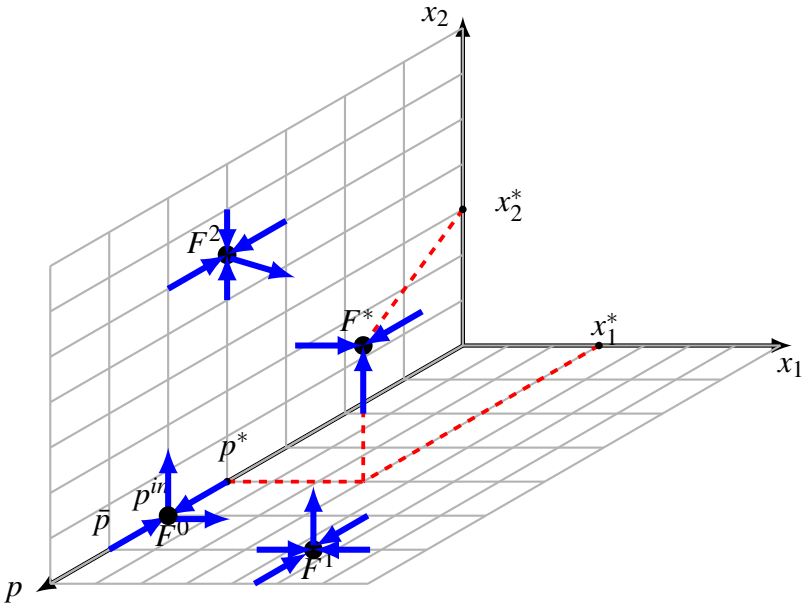

Figure 3. Equilibria configuration. The three equilibria F^0, F^1 and F^2 are saddle points and F^* is an asymptotically stable steady state.

Consider a solution $\vec{\mathbf{z}} = (p(t), x_1(t), x_2(t))$ with an initialization $\vec{\mathbf{z}}(0) = (p(0), x_1(0), x_2(0))$ with $p(0) > 0$, $x_1(0) > 0$ and $x_2(0) > 0$ as nonnegative constants. We denoted by $\gamma^+(\vec{\mathbf{z}}(0))$, the positive semi-orbit through $\vec{\mathbf{z}}(0)$ and $\omega = \omega(\gamma^+(\vec{\mathbf{z}}(0)))$, the omega limit set of $\gamma^+(\vec{\mathbf{z}}(0))$. Let us now prove that ω has no points on the faces of $\mathscr{S}$.

- Let us suppose that $F^0 \in \omega$, which means that there exists $z^* \neq F^0$ in $\omega \cap W^s(F^0) \backslash \{F^0\}$. Since the stable manifold of F^0 denoted by $W^s(F^0)$ is one-dimensional, restricted to the p-axis, as a consequence, the full orbit through z^* (belonging to ω) will be unbounded and this contradicts the existence of z^*.
- Let us suppose that $F^1 \in \omega$ (respectively, $F^2 \in \omega$). F^1 (respectively, F^2) is a saddle point with a stable manifold, $W^s(F^1)$ (respectively, $W^s(F^2)$) of dimension two, restricted to the px_1-plane (respectively, px_2-plane). Therefore, $\{F^1\}$ (respectively, $\{F^2\}$) is not the entire omega limit set ω. Using Butler-McGehee lemma [32], there exists a point $z^* \neq F^1$ (respectively, $z^* \neq F^2$) inside $\omega \cap W^s(F^1) \backslash \{F^1\}$ (respectively, $\omega \cap W^s(F^2) \backslash \{F^1\}$). Since $W^s(F^1)$ (respectively, $W^s(F^2)$) lies entirely in the px_1-plane (respectively, px_2-plane), and since the entire orbit through z^* is in ω, this orbit is unbounded, which contradicts the fact that F^1 (respectively, F^2) is inside ω.

Consider $\underline{\mathbf{z}} = (\underline{\mathrm{p}}(t), \underline{\mathrm{x}}_1(t), \underline{\mathrm{x}}_2(t))$ and suppose that least $\underline{\mathrm{p}}(t)$, $\underline{\mathrm{x}}_1(t)$ or $\underline{\mathrm{x}}_2(t)$ is zero with $\underline{\mathbf{z}} \in \omega$. This leads with the fact that the entire orbit through $\underline{\mathbf{z}}$ will be in ω. Therefore, the orbit will be entirely in one of the faces px_1, x_1x_2 or px_2, then it will converge to one of the boundary equilibria. This means

that one of equilibria is in ω, which contradicts what we have just shown above. Thus, all components of the solution are greater than zero.

$$\liminf_{t\to\infty} p(t) > 0,\ \liminf_{t\to\infty} x_1(t) > 0 \ \text{ and } \ \liminf_{t\to\infty} x_2(t) > 0,$$

and the dynamics (4.1) is persistent (see [14, 18, 20, 35] for other applications). □

5.4. Uniform persistence for the reduced dynamics

In several cases of biological models, the persistence and uniform persistence [36] are associated. Here, we will apply the theory given in [36], proving that dynamics $(\mathscr{E})$ admitting $\mathbb{R}^3_+$ and $\partial\mathbb{R}^3_+$ as invariant sets, then, $(\mathscr{E})$ is uniformly persistent if we have

1) $(\mathscr{E})$ is weakly persistent,
2) $(\partial\mathscr{E})$ is acyclic; $(\partial\mathscr{E})$ be the restriction of $(\mathscr{E})$ to $\partial\mathbb{R}^3_+$,
3) $(\mathscr{E})$ is dissipative,
4) $(\partial\mathscr{E})$ is isolated.

Let the dynamics (4.1) be a candidate of $(\mathscr{E})$ on Σ. By using the theory given in [36], if $\partial\Sigma$ can be written in the form $\partial\Sigma = \Sigma_1 \cup \Sigma_2$ such that $(\mathscr{E})$ is invariant on Σ_1 but attracting Σ_2 inside the interior of Σ by restricting the dynamics $(\mathscr{E})$ to Σ_1 to satisfy the Conditions 2 and 4, the one can easily see the satisfaction of Condition 1 and the satisfaction of Condition 3 according to Theorem 3. Furthermore, since all boundary equilibria are hyperbolic forming a covering of the omega limit sets of Σ_1, then there is the satisfaction of Condition 2. Moreover, since the boundary equilibria are not linked cyclically, then there is the satisfaction of condition 4. Thus, the uniform persistence of dynamics (4.1) is satisfied.

Theorem 4. *The reduced model (4.1) is uniformly persistent;* $\exists\ \delta > 0$ *satisfying*

$$\min\left(\liminf_{t\to\infty} p(t), \liminf_{t\to\infty} x_1(t), \liminf_{t\to\infty} x_2(t)\right) > \delta.$$

5.5. Uniform persistence for the main dynamics

Let us now reconsider the dynamics (2.2) modeling a foodweb associated to the second and third stages of the anaerobic degradation process under perfect mixing conditions conducted by the acetogenic and the hydrogenotrophic-methanogenic bacteria and taking into account of the leachate recirculation. Assume that the system (2.2) satisfies Assumptions H1–H6. Note that system (2.2) admits E^0, E^1, E^2 and E^* as steady states. E^0, E^1 and E^2 are saddle points, however, E^* is locally asymptotically stable.

Let us prove the uniform persistence of dynamics (2.2). Let $\vec{\mathbf{y}}_{\mathbf{0}} = (s_1(0), s_2(0), p(0), x_1(0), x_2(0))$ with $s_1(0) \geq 0, s_2(0) \geq 0, p(0) \geq 0, x_1(0) \geq 0$ and $x_2(0) \geq 0$, then $\omega(\vec{\mathbf{y}}_{\mathbf{0}}) \in \Sigma$. Moreover, suppose that $\exists\ \vec{\tau} \in \mathbb{R}^5_+ \setminus \Sigma$ such that the trajectory converges to $\vec{\tau}$, which is impossible because Σ is an attractor of all solutions according to Proposition 1. Furthermore, assume that $\omega(\vec{\mathbf{y}}_{\mathbf{0}})$ contains a point from one of the faces i.e., one of the variable p, x_1 or x_2 is equal to zero. Thus, the entire trajectory through this point should be entirely inside $\omega(\vec{\mathbf{y}}_{\mathbf{0}})$. Therefore, the omega limit set $\omega(\vec{\mathbf{y}}_{\mathbf{0}})$ must be entirely inside Σ.

Theorem 5. *The main model (2.2) is uniformly persistent, in the sense that there exists* $\theta > 0$ *satisfying*

$$\min\left(\liminf_{t\to\infty} s_1(t), \liminf_{t\to\infty} s_2(t), \liminf_{t\to\infty} p(t), \liminf_{t\to\infty} x_1(t), \liminf_{t\to\infty} x_2(t)\right) > \theta.$$

For the next section and for simplicity, we will consider the case where the function h is linear, i.e., $h(u) = \bar{h}u$ where $\bar{h} > 0$ is a constant.

6. Optimal strategy for leachate recirculation

Anaerobic digestion, also called "methanization", is the degradation of organic matter by microorganisms in a closed environment devoid of oxygen. The anaerobic digestion produces biogas (consisting mainly of methane and carbon dioxide). The leachate recirculation permits to transform insoluble organic matter into a soluble one. The goal of this section is to propose an optimal strategy for leachate recirculation to reduce the organic matter $(s_1(t), s_2(t))$ and by keeping a limitation of the costs of the recirculation operation $u(t)$ during the process. A previous strategy was applied to this model but without leachate recirculation, where the goal was to maximize the biogas production [29]. We will consider an objective functional reflecting the minimization of substrate in its two forms $(s_1(t), s_2(t))$, which leads to maximizing the methane production.

Let us consider a time-varying control function $u(t)$ expressing the recirculation costs. Assume that μ_1 and μ_2 are globally Lipschitz where the upper bounds are given by $\bar{\mu}_1 = \sup_{s_2,p>0} \mu_1(s_2,p)$ and $\bar{\mu}_2 = \sup_{p>0} \mu_2(p)$ and Lipschitz constants L_1 and L_2, respectively.

The admissible control set is given by

$$\mathbf{P_{ad}} = \{u(t) : 0 \leq u^{\min} \leq u(t) \leq u^{\max}, 0 \leq t \leq T, u(t) \text{ is Lebesgue measurable}\},$$

which minimizes the following objective functional:

$$J(u) = \frac{\alpha_1}{2}\int_0^T s_1^2(t)\,dt + \frac{\alpha_2}{2}\int_0^T s_2^2(t)\,dt + \frac{\beta}{2}\int_0^T u^2(t)\,dt.$$

By choosing appropriate positive balancing constants α_1, α_2 and β, the goal is to minimize the quantity of the substrate in its two forms and also the cost of the control. We use standard results [37] to show the existence of both the optimal control and the corresponding states. For $\varpi = (s_1, s_2, p, x_1, x_2)^t$, dynamics (2.2) can be expressed as follows:

$$\dot{\varpi} = \sigma\varpi + \rho(\varpi) = \upsilon(\varpi) \tag{6.1}$$

with $\sigma = -DI_4$ and $\rho(\varpi) = \begin{pmatrix} Ds_1^{in} - \bar{h}ug(s_1) \\ Ds_2^{in} + \bar{h}ug(s_1) - 2\mu_1(s_2,p)x_1 \\ Dp^{in} - \mu_2(p)x_2 + \mu_1(s_2,p)x_1 \\ \mu_1(s_2,p)x_1 \\ \mu_2(p)x_2 \end{pmatrix}$, where I_4 is the 4×4 identity matrix.

Note that ρ satisfies

$$\begin{aligned}
\left\|\rho(\varpi')-\rho(\varpi)\right\|_1 &= \left|\bar{h}ug(s_1')-\bar{h}ug(s_1)\right|+\left|\bar{h}ug(s_1')-\bar{h}ug(s_1)+2(\mu_1(s_2',p')x_1'-\mu_1(s_2,p)x_1)\right| \\
&\quad +\left|\mu_1(s_2',p')x_1'-\mu_1(s_2,p)x_1+\mu_2(p)x_2-\mu_2(p')x_2'\right|+\left|\mu_2(p')x_2'-\mu_2(p)x_2\right| \\
&\leq 2\bar{h}u\left|g(s_1')-g(s_1)\right|+3\left|\mu_1(s_2',p')x_1'-\mu_1(s_2,p)x_1\right|+2\left|\mu_2(p)x_2-\mu_2(p')x_2'\right| \\
&\leq 2\bar{h}u^{max}|s_1'-s_1|+3\bar{\mu}_1|x_1'-x_1|+3(s_1^{in}+s_2^{in}+p^{in})L_1\left|(s_2',p')-(s_2,p)\right| \\
&\quad +2\bar{\mu}_2|x_2'-x_2|+2(s_1^{in}+s_2^{in}+p^{in})L_2\left|p'-p\right| \\
&\leq M\left\|\varpi_1-\varpi_2\right\|_1,
\end{aligned}$$

where $M=\max(2\bar{h}u^{max},3\bar{\mu}_1,3(s_1^{in}+s_2^{in}+p^{in})L_1,2\bar{\mu}_2,2(s_1^{in}+s_2^{in}+p^{in})L_2)$. Since $\left\|\sigma\varpi_1-\sigma\varpi_2\right\|_1\leq D\left\|\varpi_1-\varpi_2\right\|_1$, then $\left\|\upsilon(\varpi_1)-\upsilon(\varpi_2)\right\|_1\leq K\left\|\varpi_1-\varpi_2\right\|_1$ with $K=\max(M,D)$ and, therefore, υ is a uniformly Lipschitz continuous function.

Therefore, system (6.1) admits a unique solution. By applying Pontryagin's Maximum principle [37–39], the optimal control problem for dynamics (6.1) subject to the minimization of the objective functional J can be formulated in terms of the Hamiltonian function

$$\begin{aligned}
H &= \frac{\alpha_1}{2}s_1^2+\frac{\alpha_2}{2}s_2^2+\frac{\beta}{2}u^2+\lambda_1\dot{s}_1+\lambda_2\dot{s}_2+\lambda_3\dot{p}+\lambda_4\dot{x}_1+\lambda_5\dot{x}_2 \\
&= \frac{\alpha_1}{2}s_1^2+\frac{\alpha_2}{2}s_2^2+\frac{\beta}{2}u^2 \\
&\quad +\lambda_1(D(s_1^{in}-s_1)-\bar{h}ug(s_1)) \\
&\quad +\lambda_2(D(s_2^{in}-s_2)+\bar{h}ug(s_1)-2\mu_1(s_2,p)x_1) \\
&\quad +\lambda_3(D(p^{in}-p)-\mu_2(p)x_2+\mu_1(s_2,p)x_1) \\
&\quad +\lambda_4(\mu_1(s_2,p)x_1-Dx_1) \\
&\quad +\lambda_5(\mu_2(p)x_2-Dx_2).
\end{aligned} \tag{6.2}$$

For a given optimal control u, there exists adjoint functions $\lambda_1,\lambda_2,\lambda_3,\lambda_4$ and λ_5 corresponding to the states s_1,s_2,p,x_1 and x_2 that solve the adjoint system given hereafter,

$$\begin{cases}
\dot{\lambda}_1 &= -\dfrac{\partial H}{\partial s_1}=-\alpha_1 s_1+\lambda_1(D+\bar{h}ug'(s_1))-\lambda_2\bar{h}ug'(s_1), \\
\dot{\lambda}_2 &= -\dfrac{\partial H}{\partial s_2}=-\alpha_2 s_2+\lambda_2(D+2\dfrac{\partial\mu_1(s_2,p)}{\partial s_2}x_1)-(\lambda_3+\lambda_4)\dfrac{\partial\mu_1(s_2,p)}{\partial s_2}x_1, \\
\dot{\lambda}_3 &= -\dfrac{\partial H}{\partial p}=(2\lambda_2-\lambda_4)\dfrac{\partial\mu_1(s_2,p)}{\partial p}x_1+\lambda_3\Big(D+\mu_2'(p)x_2-\dfrac{\partial\mu_1(s_2,p)}{\partial p}x_1\Big)-\lambda_5\mu_2'(p)x_2, \\
\dot{\lambda}_4 &= -\dfrac{\partial H}{\partial x_1}=(2\lambda_2-\lambda_3)\mu_1(s_2,p)-\lambda_4(\mu_1(s_2,p)-D), \\
\dot{\lambda}_5 &= -\dfrac{\partial H}{\partial x_2}=\lambda_3\mu_2(p)-\lambda_5(\mu_2(p)-D),
\end{cases}$$

with $\lambda_1(T)=0$, $\lambda_2(T)=0$, $\lambda_3(T)=0$, $\lambda_4(T)=0$ and $\lambda_5(T)=0$.

The Hamiltonian is minimized with respect to the control variable at u. The derivative of the Hamiltonian is given by $\dfrac{\partial H}{\partial u}=\beta u-\lambda_1\bar{h}g(s_1)+\bar{h}\lambda_2 g(s_1)=\beta u+\bar{h}(\lambda_2-\lambda_1)g(s_1)$.

Therefore, $\dfrac{\partial H}{\partial u} = 0$ admits the solution $u^*(t) = \dfrac{\bar{h}}{\beta}(\lambda_1 - \lambda_2)g(s_1)$ provided that $\beta \neq 0$ and

$$0 < u^{\min} \leq \frac{\bar{h}}{\beta}(\lambda_1 - \lambda_2)g(s_1) \leq u^{\max}.$$

To summarize, the control characterization is:

$$\begin{cases} \text{if } \dfrac{\partial H}{\partial u} < 0 \text{ at } t, \text{ then } u(t) = u^{\max}, \\ \text{if } \dfrac{\partial H}{\partial u} > 0 \text{ at } t, \text{ then } u(t) = u^{\min}, \\ \text{if } \dfrac{\partial H}{\partial u} = 0 \text{ at } t, \text{ then } u(t) = u^*(t) = \dfrac{\bar{h}}{\beta}(\lambda_1 - \lambda_2)g(s_1). \end{cases}$$

7. Numerical simulations

We confirm the theoretical results using Holling's functions type II as candidates for the growth rates, the solubilization rate and the hydrolysis rate.

$$\mu_1(s,p) = \frac{\bar{\mu}_1 s}{(k_s + s)(k_p + p)}, \mu_2(p) = \frac{\bar{\mu}_2 p}{k_2 + p}, g(s) = \frac{\bar{g}s}{k_3 + s} \text{ and } h(u) = \bar{h}u$$

where k_s, k_p, k_2, k_3, $\bar{\mu}_1$, $\bar{\mu}_2, \bar{g}$ and $\bar{h}$ are positive constants and are given with the model parameters in Table 2. We used Holling's functions type II (or also Monod functions) as typical examples [40, 41] since they are nonlinear and satisfied all our assumptions on either growth rates or the solubilization and the hydrolysis rates.

Table 2. Some parameters values considered for the numerical simulation. Note that these values have no biological meaning.

Parameter	$\bar{\mu}_1$	$\bar{\mu}_2$	$\bar{g}$	$\bar{h}$	k_s	k_p	k_2	k_3	s_1^{in}	s_2^{in}	p^{in}
Value	8	12	1.1	1	1	20	13	6	6	3	4

7.1. Numerical simulation for the main dynamics (2.2)

We give five numerical examples for the main dynamics (2.2) for a fixed leachate recirculation rate u. The first example satisfies the Assumptions H1 to H6 for a dilution rate $D = 0.25$ and a leachate recirculation rate $u = 2$, which ensures the uniform persistence of the dynamics (2.2) according to Theorem 5, thus, the coexistence of both bacteria as seen in Figure 4 (left). As expected, the trajectories filling the whole positive cone converge to the positive steady state (Figure 4, right).

The second example is the same as the first one, except by taking a leachate recirculation rate $u = 4$. Again, the uniform persistence of the dynamics (2.2) is satisfied. Both bacteria persist as seen in Figure 5 (left). Note that by increasing the leachate recirculation rate u the bacteria concentrations increase however the substrate concentrations decrease.

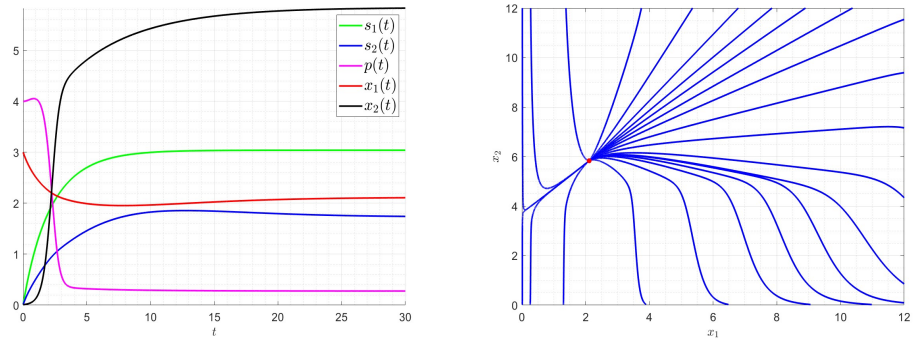

Figure 4. Behavior of dynamics (2.2); the components behavior (left) and the $x_1 - x_2$ behavior (right) for $u = 2$ and $D = 0.25$. Both species persist.

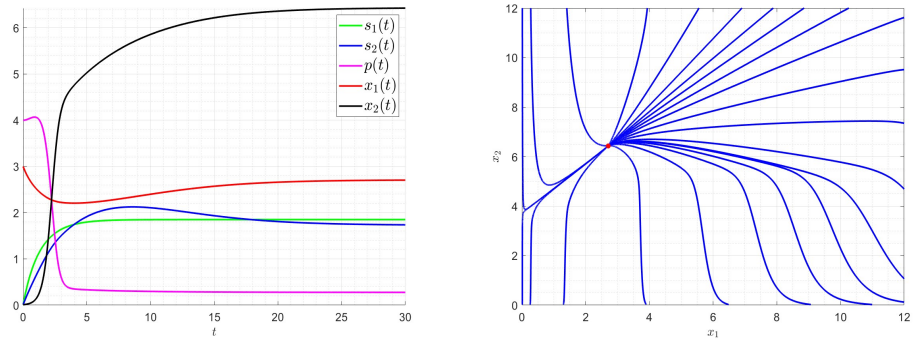

Figure 5. Behavior of dynamics (2.2); the components behavior (left) and the $x_1 - x_2$ behavior (right) for $u = 4$ and $D = 0.25$. Both species persist.

In Figure 6, the dilution rate is given by $D = 1$, which satisfies only Assumptions H2 to H6 and does not satisfy Assumptions H1. Therefore, only species two can persist and the global stability of the equilibrium point E^2. The trajectories filling the whole positive cone converge to the point where $x_1 = 0$ (Figure 6, right).

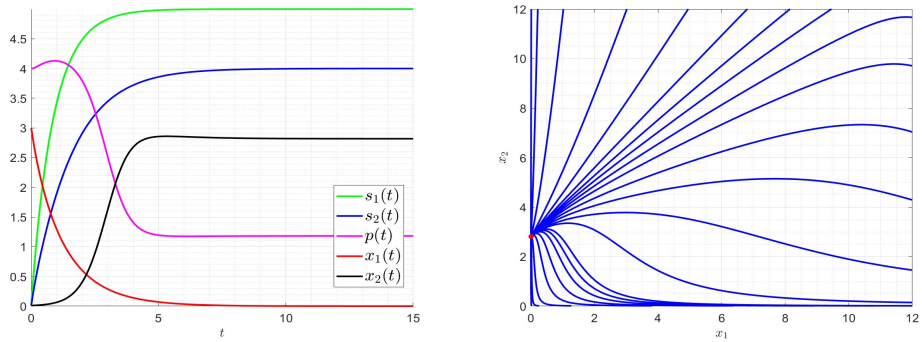

Figure 6. Behavior of dynamics (2.2); the components behavior (left) and the $x_1 - x_2$ behavior (right) for $D = 1$. The trajectory converges to the steady state E^2.

In Figure 7, the dilution rate is given by $D = 0.48$. For the specific values $\bar{\mu}_1 = 12$, $\bar{\mu}_2 = 4$, $s_2^{in} = 6$ and $p^{in} = 1$, only species one can persist and the global stability of the equilibrium point E^1. The trajectories filling the whole positive cone converge to the point where $x_2 = 0$ (Figure 7, right).

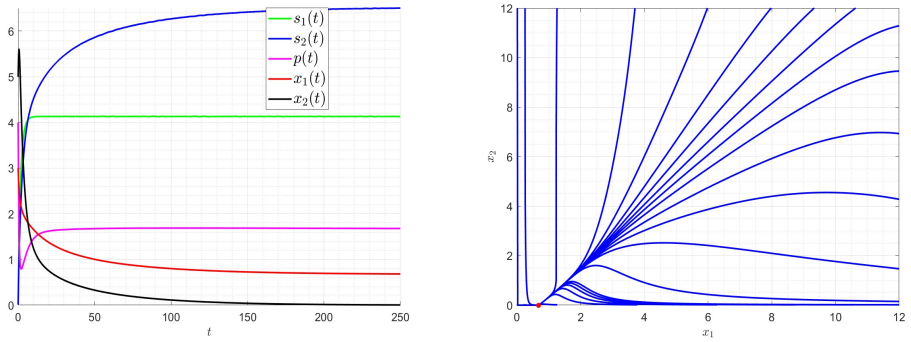

Figure 7. Behavior of dynamics (2.2); the components behavior (left) and the $x_1 - x_2$ behavior (right) for the specific following values $D = 0.48$, $\bar{\mu}_1 = 12$, $\bar{\mu}_2 = 4$, $s_2^{in} = 6$ and $p^{in} = 1$. The trajectory converges to the steady state E^1.

In Figure 8, the dilution rate is given by $D = 3$ which does not satisfy Assumptions H1 and H5. Therefore, no one of the two species can persist and the global stability of the trivial equilibrium point E^0, where all species go to extinction. The trajectories filling the whole positive cone converge to the origin (Figure 8, right).

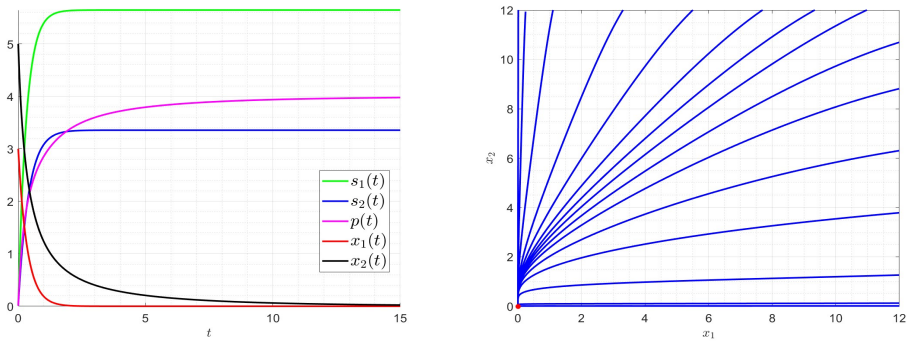

Figure 8. Behavior of dynamics (2.2); the components behavior (left) and the $x_1 - x_2$ behavior (right) for $D = 3$. The trajectory converges to the steady state E^0.

7.2. Numerical simulation for the control problem

In this section, we aim to apply the optimal strategy to reduce the total organic matter and keep the costs minimal. We keep all parameters the same as in the previous section and consider only a time-varying control function $u(t)$ expressing the recirculation costs. We impose the following bounds on the control $u^{\min} = 0.05$ and $u^{\max} = 20$ with the control initial condition $u(0) = 2$ as it is fixed for the main dynamics (2.2) in the previous section, which permits to compare and conclude on the efficiency of the optimal strategy. We choose the initial state as $x_0 = (6, 5, 7, 0.01, 0.01)$ with a final time $T = 140$. Concerning the numerical resolution of the control problem, we used a numerical scheme that improves the Gauss-Seidel-like implicit finite-difference method where we applied a first-

order backward-difference for the adjoint variables (see Appendix 8 for more details and [42–44] for other applications).

As it is seen in Figures 9–11, the curve of the optimal solution looks smooth. When increasing the value of β, the asymptotic values of the control decrease and need more time to converge. However it increases when increasing the values of α_1 and α_1 but with the same time of convergence. The optimal strategy permits to increase both, soluble and insoluble organic matter with optimal control values.

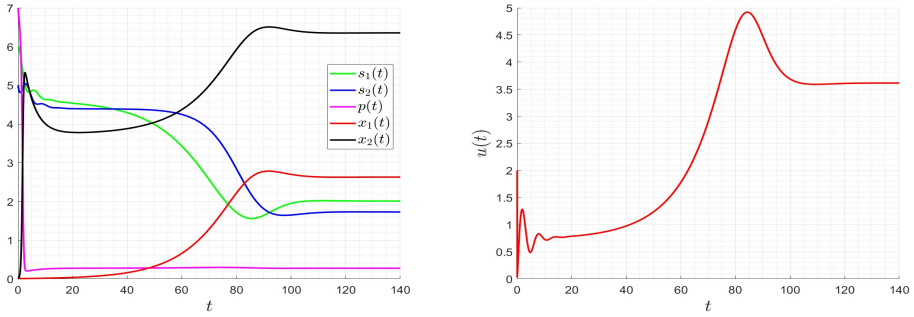

Figure 9. State variable (left) and control (right) behavior for $\alpha_1 = 1$, $\alpha_2 = 1$, $\beta = 1$, $D = 0.25$.

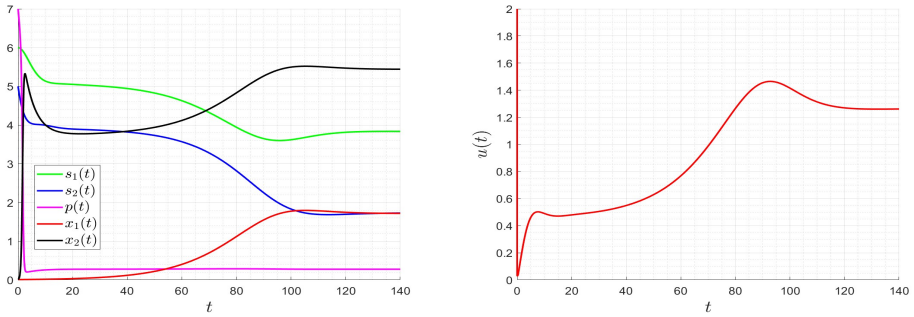

Figure 10. State variable (left) and control (right) behavior for $\alpha_1 = 1$, $\alpha_2 = 1$, $\beta = 10$, $D = 0.25$.

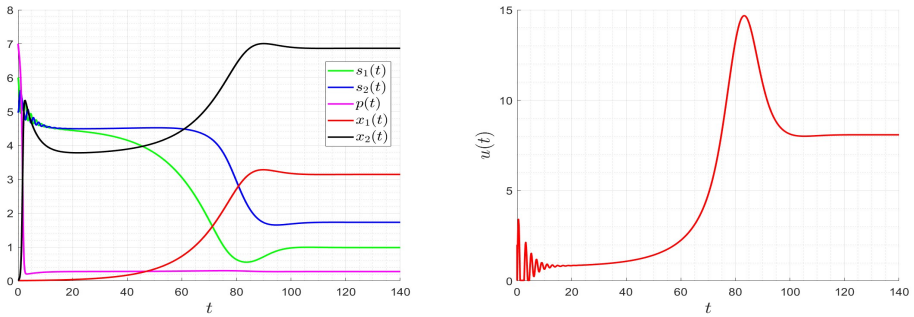

Figure 11. State variable (left) and control (right) behavior for $\alpha_1 = 10$, $\alpha_2 = 10$, $\beta = 1$, $D = 0.25$.

8. Conclusions

We presented a simple five-dimensional dynamical system modeling a foodweb associated to the second and third stages of the anaerobic degradation process under perfect mixing conditions conducted by the acetogenic and the hydrogenotrophic-methanogenic bacteria, taking into account the leachate recirculation. We considered two component substrates: The first one was insoluble transformed under a solubilization process, and the second one was a soluble component that was degraded by an acetogenic bacteria to produce the hydrogen, which is an essential nutriment for the hydrogenotrophic-methanogenic bacteria. We reduced the system to a three-dimensional one, we studied the local stability and, therefore, we applied the persistence theory to conclude on the persistence of both species. Moreover, we discussed an optimal strategy for the leachate recirculation in order to minimize the organic matter and keep the operation costs for monitoring the effects of leachate recirculation minimal. We presented some numerical simulations, confirming the theoretical findings for both direct and control problems.

Use of AI tools declaration

The authors declare they have not used Artificial Intelligence (AI) tools in the creation of this article.

Funding

This work was funded by the University of Jeddah, Jeddah, Saudi Arabia, under grant No. UJ-23-DR-113.

Acknowledgements

This work was funded by the University of Jeddah, Jeddah, Saudi Arabia, under grant No. UJ-23-DR-113. Therefore, the author thanks the University of Jeddah for its technical and financial support.

The author is also grateful to the unknown referees for many constructive suggestions, which helped to improve the presentation of the paper.

Conflict of interest

The author declares no conflict of interest.

References

1. N. A. F. Zamrisham, A. M. Wahab, A. Zainal, D. Karadag, D. Bhutada, S. Suhartini, et al., State of the art in anaerobic treatment of landfill leachate: A review on integrated system, additive substances, and machine learning application, *Water*, **15** (2023), 1303. https://doi.org/10.3390/w15071303
2. K. Waszkielis, I. Bialobrzewski, K. Bulkowska, Application of anaerobic digestion model No.1 for simulating fermentation of maize silage, pig manure, cattle manure and digestate in the full-scale biogas plant, *Fuel*, **317** (2022), 123491. https://doi.org/10.1016/j.fuel.2022.123491

3. S. Kusch, H. Oechsner, T. Jungbluth, Effect of various leachate recirculation strategies on batch anaerobic digestion of solid substrates, *Int. J. Environ. Waste Manag.*, **9** (2012), 69–88. https://doi.org/10.1504/IJEWM.2012.044161
4. P. J. He, X. Qu, L. M. Shao, G. J. Li, D. J. Lee, Leachate pretreatment for enhancing organic matter conversion in landfill bioreactor, *J. Hazard. Mater.*, **142** (2007), 288–296. https://doi.org/10.1016/j.jhazmat.2006.08.017
5. D. R. Reinhart, B. A. Al-Yousfi, The impact of leachate recirculation on municipal solid waste landfill operating characteristics, *Waste Manag. Res.*, **14** (1996), 337–346. https://doi.org/10.1006/wmre.1996.0035
6. H. Benbelkacem, R. Bayard, A. Abdelhay, Y. Zhang, R. Gourdon, Effect of leachate injection modes on municipal solid waste degradation in anaerobic bioreactor, *Bioresource Technol.*, **101** (2010), 5206–5212. https://doi.org/10.1016/j.biortech.2010.02.049
7. L. Liu, H. Xiong, J. Ma, S. Ge, X. Yu, G. Zeng, Leachate recirculation for enhancing methane generation within field site in China, *J. Chem.*, **2018**, (2018), 9056561. https://doi.org/10.1155/2018/9056561
8. L. Luo, S. Xu, J. Liang, J. Zhao, J. W. C. Wong, Mechanistic study of the effect of leachate recirculation ratios on the carboxylic acid productions during a two-phase food waste anaerobic digestion, *Chem. Eng. J.*, **453** (2023), 139800. https://doi.org/10.1016/j.cej.2022.139800
9. IWA Task Group for Mathematical Modelling of Anaerobic Digestion Processes, *Anaerobic digestion No.1 (ADM1)*, London, UK: IWA publishing, 2005. https://doi.org/10.2166/9781780403052
10. D. J. Batstone, J. Keller, I. Angelidaki, S. V. Kalyuzhnyi, S. G. Pavlostathis, A. Rozzi, et al., The IWA anaerobic digestion model No 1 (ADM1), *Water Sci. Technol.*, **45** (2002), 65–73. https://doi.org/10.2166/wst.2002.0292
11. X. Zhao, L. Li, D. Wu, T. Xiao, Y. Ma, X. Peng, Modified anaerobic digestion model No. 1 for modeling methane production from food waste in batch and semi-continuous anaerobic digestions, *Bioresoure Technol.*, **271** (2019), 109–117. https://doi.org/10.1016/j.biortech.2018.09.091
12. A. Bornhoft, R. Hanke-Rauschenbach, K. Sundmacher, Steady-state analysis of the anaerobic digestion model No.1 (ADM1), *Nonlinear Dyn.*, **73** (2013), 535–549. https://doi.org/10.1007/s11071-013-0807-x
13. M. J. Wade, R. W. Pattinson, N. G. Parker, J. Dolfing, Emergent behaviour in a chlorophenol35 mineralising three-tiered microbial 'food web', *J. Theor. Biol.*, **389** (2016), 171–186. https://doi.org/10.1016/j.jtbi.2015.10.032
14. A. A. Alsolami, M. El Hajji, Mathematical analysis of a bacterial competition in a continuous reactor in the presence of a virus, *Mathematics*, **11** (2023), 883. https://doi.org/10.3390/math11040883
15. A. H. Albargi, M. El Hajji, Bacterial competition in the presence of a virus in a chemostat, *Mathematics*, **11** (2023), 3530. https://doi.org/10.3390/math11163530

16. G. Lyberatos, I. V. Skiadas, Modelling of anaerobic digestion–A review, *Glob. Nest J.*, **1** (1999), 63–76. https://doi.org/10.30955/gnj.000112

17. M. Weedermann, G. Seo, G. Wolkowicz, Mathematical model of anaerobic digestion in a chemostat: Effects of syntrophy and inhibition, *J. Biol. Dyn.*, **7** (2013), 59–85. https://doi.org/10.1080/17513758.2012.755573

18. S. Sobieszek, M. J. Wade, G. S. K. Wolkowicz, Rich dynamics of a three-tiered anaerobic food-web in a chemostat with multiple substrate inflow, *Math. Biosci. Eng.*, **17** (2020), 7045–7073. https://doi.org/10.3934/mbe.2020363

19. T. Bayen, G. Pedro, On the steady state optimization of the biogas production in a two-stage anaerobic digestion model, *J. Math. Biol.*, **78** (2019), 1067–1087. https://doi.org/10.1007/s00285-018-1301-3

20. M. El Hajji, N. Chorfi, M. Jleli, Mathematical modelling and analysis for a three-tiered microbial food web in a chemostat, *Electron. J. Differ. Equ.*, **2017** (2017), 1–13.

21. M. Bisi, M. Groppi, G. Martaló, R. Travaglini, Optimal control of leachate recirculation for anaerobic processes in landfills, *Discrete Cont. Dyn. Syst.-B*, **26** (2021), 2957–2976. https://doi.org/10.3934/dcdsb.2020215

22. O. Laraj, N. El Khattabi, A. Rapaport, Mathematical model of anaerobic digestion with leachate recirculation, hal-03714305f.

23. M. El Hajji, F. Mazenc, J. Harmand, A mathematical study of a syntrophic relationship of a model of anaerobic digestion process, *Math. Biosci. Eng.*, **7** (2010), 641–656. https://doi.org/10.3934/mbe.2010.7.641

24. T. Sari, M. El Hajji, J. Harmand, The mathematical analysis of a syntrophic relationship between two microbial species in a chemostat, *Math. Biosci. Eng.*, **9** (2012), 627–645. https://doi.org/10.3934/mbe.2012.9.627

25. A. Xu, J. Dolfing, T. Curtis, G. Montague, E. Martin, Maintenance affects the stability of a two-tiered microbial 'food chain'? *J. Theor. Biol.*, **276** (2011), 35–41. https://doi.org/10.1016/j.jtbi.2011.01.026

26. T. Sari, J. Harmand, A model of a syntrophic relationship between two microbial species in a chemostat including maintenance, *Math. Biosci.*, **275** (2016), 1–9. https://doi.org/10.1016/j.mbs.2016.02.008

27. Y. Daoud, N. Abdellatif, T. Sari, J. Harmand, Steady state analysis of a syntrophic model: The effect of a new input substrate concentration, *Math. Model. Nat. Phenom.*, **13** (2018), 31. https://doi.org/10.1051/mmnp/2018037

28. R. Fekih-Salem, Y. Daoud, N. Abdellatif, T. Sari, A mathematical model of anaerobic digestion with syntrophic relationship, substrate inhibition and distinct removal rates, *SIAM J. Appl. Dyn. Syst.*, **20** (2021), 1621–1654. https://doi.org/10.1137/20M1376480

29. A. H. Albargi, M. El Hajji, Mathematical analysis of a two-tiered microbial food-web model for the anaerobic digestion process, *Math. Biosci. Eng.*, **20** (2023), 6591–6611. https://doi.org/10.3934/mbe.2023283

30. R. Saidi, P. P. Liebgott, H. Gannoun, L. B. Gaida, B. Miladi, M. Hamdi, et al., Biohydrogen production from hyperthermophilic anaerobic digestion of fruit and vegetable wastes in seawater: Simplification of the culture medium of thermotoga maritima, *Waste Manage.*, **71** (2018), 474–484. https://doi.org/10.1016/j.wasman.2017.09.042

31. M. El Hajji, How can inter-specific interferences explain coexistence or confirm the competitive exclusion principle in a chemostat? *Int. J. Biomath.*, **11** (2018), 1850111. https://doi.org/10.1142/S1793524518501115

32. H. L. Smith, P. Waltman, *The theory of the chemostat: Dynamics of microbial competition*, Cambridge University Press, 1995. https://doi.org/10.1017/CBO9780511530043

33. H. R. Thieme, Convergence results and a Poincaré-Bendixson trichotomy for asymptotically autonomous differential equations, *J. Math. Biol.*, **30** (1992), 755–763. https://doi.org/10.1007/BF00173267

34. H. R. Thieme, Asymptotically autonomous differential equations in the plane, *Rocky Mountain J. Math.*, **24** (1993), 351–380. https://doi.org/10.1216/rmjm/1181072470

35. M. El Hajji, Periodic solutions for chikungunya virus dynamics in a seasonal environment with a general incidence rate, *AIMS Mathematics*, **8** (2023), 24888–24913. https://doi.org/10.3934/math.20231269

36. G. Butler, H. I. Freedman, P. Waltman, Uniformly persistent systems, *Proc. Amer. Math. Soc.*, **96** (1986), 425–429. https://doi.org/10.1090/S0002-9939-1986-0822433-4

37. W. Fleming, R. Rishel, *Deterministic and stochastic optimal control*, New York: Springer Verlag, 1975. https://doi.org/10.1007/978-1-4612-6380-7

38. S. Lenhart, J. T. Workman, *Optimal control applied to biological models*, Chapman and Hall/CRC, 2007. https://doi.org/10.1201/9781420011418

39. L. S. Pontryagin, *Mathematical theory of optimal processes*, Routledge, 1987. https://doi.org/10.1201/9780203749319

40. J. Monod, Croissance des populations bactériennes en fonction de la concentration de l'aliment hydrocarboné, *C. R. Acad. Sci.*, **212** (1941), 771–773.

41. J. R. Lobry, J. P. Flandrois, G. Carret, A. Pave, Monod's bacterial growth model revisited, *Bull. Math. Biol.*, **54** (1992), 117–122. https://doi.org/10.1007/BF02458623

42. M. El Hajji, Modelling and optimal control for Chikungunya disease, *Theory Biosci.*, **140** (2021), 27–44. https://doi.org/10.1007/s12064-020-00324-4

43. M. El Hajji, A. Zaghdani, S. Sayari, Mathematical analysis and optimal control for Chikungunya virus with two routes of infection with nonlinear incidence rate, *Int. J. Biomath.*, **15** (2022), 2150088. https://doi.org/10.1142/S1793524521500881

44. M. El Hajji, S. Sayari, A. Zaghdani, Mathematical analysis of an SIR epidemic model in a continuous reactor–deterministic and probabilistic approaches, *J. Korean Math. Soc.*, **58** (2021), 45–67. https://doi.org/10.4134/JKMS.j190788

Appendix A

Appropriated scheme for the control problem

The time interval $[0,T]$ is discretesized as follows: $[0,T] = \bigcup_{n=0}^{N-1} [t_n, t_{n+1}], \quad t_n = ndt, \quad dt = T/N.$

Let s_1^n, s_2^n, p^n, x_1^n, x_2^n, λ_1^n, λ_2^n, λ_3^n, λ_4^n, λ_5^n and u^n be an approximation of $s_1(t)$, $s_2(t)$, $p(t)$, $x_1(t)$, $x_2(t)$, $\lambda_1(t)$, $\lambda_2(t)$, $\lambda_3(t)$, $\lambda_4(t)$, $\lambda_5(t)$ and the control $u(t)$ at the time t_n, s_1^0, s_2^0, p^0, x_1^0, x_2^0, λ_1^0, λ_2^0, λ_3^0, λ_4^0, λ_5^0 and u^0 as the state and adjoint variables and the controls at initial time and s_1^N, s_2^N, p^N, x_1^N, x_2^N, λ_1^N, λ_2^N, λ_3^N, λ_4^N, λ_5^N and u^N as the state and adjoint variables and the control at final time T. A Gauss-Seidel-like implicit finite-difference method was created for the state variables. However, a first-order backward-difference is applied to solve the adjoint states.

$$
\begin{cases}
\dfrac{s_1^{n+1}-s_1^n}{dt} &= D(s_1^{in}-s_1^{n+1}) - \dfrac{\bar{h}u^n\bar{g}s_1^{n+1}}{k_3+s_1^n},\\
\dfrac{s_2^{n+1}-s_2^n}{dt} &= D(s_2^{in}-s_2^{n+1}) + \dfrac{\bar{h}u^n\bar{g}s_1^{n+1}}{k_3+s_1^{n+1}} - \dfrac{2\bar{\mu}_1 s_2^{n+1}x_1^n}{(k_s+s_2^n)(k_p+p^n)},\\
\dfrac{p^{n+1}-p^n}{dt} &= D(p^{in}-p^{n+1}) - \dfrac{\bar{\mu}_2 p^{n+1}x_2^n}{k_2+p^n} + \dfrac{\bar{\mu}_1 s_2^{n+1}x_1^n}{(k_s+s_2^{n+1})(k_p+p^n)},\\
\dfrac{x_1^{n+1}-x_1^n}{dt} &= \dfrac{\bar{\mu}_1 s_2^{n+1}x_1^{n+1}}{(k_s+s_2^{n+1})(k_p+p^{n+1})} - Dx_1^{n+1},\\
\dfrac{x_2^{n+1}-x_2^n}{dt} &= \dfrac{\bar{\mu}_2 p^{n+1}x_2^{n+1}}{k_2+p^{n+1}} - Dx_2^{n+1},\\
\dfrac{\lambda_1^{N-n}-\lambda_1^{N-n-1}}{dt} &= -\alpha_1 s_1^{n+1} + \lambda_1^{N-n-1}\left(D + \dfrac{\bar{h}u^n\bar{g}k_3}{(k_3+s_1^{n+1})^2}\right) - \lambda_2^{N-n}\dfrac{\bar{h}u^n\bar{g}k_3}{(k_3+s_1^{n+1})^2},\\
\dfrac{\lambda_2^{N-n}-\lambda_2^{N-n-1}}{dt} &= -\alpha_2 s_2^{n+1} + \lambda_2^{N-n-1}\left(D + \dfrac{2\bar{\mu}_1 k_s x_1^{n+1}}{(k_s+s_2^{n+1})^2(k_p+p^{n+1})}\right)\\
&\quad -(\lambda_3^{N-n}+\lambda_4^{N-n})\dfrac{\bar{\mu}_1 k_s x_1^{n+1}}{(k_s+s_2^{n+1})^2(k_p+p^{n+1})},\\
\dfrac{\lambda_3^{N-n}-\lambda_3^{N-n-1}}{dt} &= \dfrac{(\lambda_3^{N-n-1}+\lambda_4^{N-n}-2\lambda_2^{N-n-1})\bar{\mu}_1 s_2^{n+1}x_1^{n+1}}{(k_s+s_2^{n+1})(k_p+p^{n+1})^2} + D\lambda_3^{N-n-1}\\
&\quad +(\lambda_3^{N-n-1}-\lambda_5^{N-n})\dfrac{\bar{\mu}_2 k_2 x_2^{n+1}}{(k_2+p^{n+1})^2},\\
\dfrac{\lambda_4^{N-n}-\lambda_4^{N-n-1}}{dt} &= \dfrac{(2\lambda_2^{N-n-1}-\lambda_3^{N-n-1})\bar{\mu}_1 s_2^{n+1}}{(k_s+s_2^{n+1})(k_p+p^{n+1})} + \lambda_4^{N-n-1}\left(\dfrac{\bar{\mu}_1 s_2^{n+1}}{(k_s+s_2^{n+1})(k_p+p^{n+1})} - D\right),\\
\dfrac{\lambda_5^{N-n}-\lambda_5^{N-n-1}}{dt} &= \dfrac{\lambda_3^{N-n-1}\bar{\mu}_2 p^{n+1}}{k_2+p^{n+1}} - \lambda_5^{N-n-1}\left(\dfrac{\bar{\mu}_2 p^{n+1}}{k_2+p^{n+1}} - D\right).
\end{cases}
$$

Hence, u^{n+1} will be calculated as follows $u^{n+1} = \dfrac{\bar{h}}{\beta}(\lambda_1^{N-n-1} - \lambda_2^{N-n-1})g(s_1^{n+1})$, provided that $\beta \neq 0$ and $0 < u^{\min} \leq u^{n+1} \leq u^{\max}$.

The algorithm hereafter will be applied under MATLAB software.

$s_1^0 \leftarrow s_1(0), s_2^0 \leftarrow s_2(0), p^0 \leftarrow p(0), x_1^0 \leftarrow x_1(0), x_2^0 \leftarrow x_2(0), \lambda_1^N \leftarrow 0, \lambda_2^N \leftarrow 0, \lambda_3^N \leftarrow 0, \lambda_4^N \leftarrow 0, \lambda_5^N \leftarrow 0, u^0 \leftarrow u(0),$

for $n = 0$ to $N-1$ **do**

$$
\left[
\begin{array}{ll}
s_1^{n+1} \leftarrow \dfrac{s_1^n + dtDs_1^{in}}{1+dt\left(D+\dfrac{\bar{h}u^n\bar{g}}{k_3+s_1^n}\right)}, & s_2^{n+1} \leftarrow \dfrac{s_2^n + dtDs_2^{in} + dt\dfrac{\bar{h}u^n\bar{g}s_1^{n+1}}{k_3+s_1^{n+1}}}{1+dt\left(D+\dfrac{2\bar{\mu}_1 x_1^n}{(k_s+s_2^n)(k_p+p^n)}\right)}, \\
p^{n+1} \leftarrow \dfrac{p^n + dtDp^{in} + \dfrac{dt\bar{\mu}_1 s_2^{n+1}x_1^n}{(k_s+s_2^{n+1})(k_p+p^n)}}{1+dt\left(D+\dfrac{\bar{\mu}_2 x_2^n}{k_2+p^n}\right)}, & x_1^{n+1} \leftarrow \dfrac{x_1^n}{1-dt\left(\dfrac{\bar{\mu}_1 s_2^{n+1}}{(k_s+s_2^{n+1})(k_p+p^{n+1})}-D\right)}, \\
x_2^{n+1} \leftarrow \dfrac{x_2^n}{1-dt\left(\dfrac{\bar{\mu}_2 p^{n+1}}{k_2+p^{n+1}}-D\right)}, & \lambda_1^{N-n-1} \leftarrow \dfrac{\lambda_1^{N-n} - dt\left(-\alpha_1 s_1^{n+1} - \lambda_2^{N-n}\dfrac{\bar{h}u^n\bar{g}k_3}{(k_3+s_1^{n+1})^2}\right)}{1+dt\left(D+\dfrac{\bar{h}u^n\bar{g}k_3}{(k_3+s_1^{n+1})^2}\right)}, \\
\lambda_2^{N-n-1} \leftarrow \dfrac{\lambda_2^{N-n} - dt\left(-\alpha_2 s_2^{n+1} - (\lambda_3^{N-n}+\lambda_4^{N-n})\dfrac{\bar{\mu}_1 k_s x_1^{n+1}}{(k_s+s_2^{n+1})^2(k_p+p^{n+1})}\right)}{1+dt\left(D+\dfrac{2\bar{\mu}_1 k_s x_1^{n+1}}{(k_s+s_2^{n+1})^2(k_p+p^{n+1})}\right)}, & \\
\lambda_3^{N-n-1} \leftarrow \dfrac{\lambda_3^{N-n} - dt\left(\dfrac{(\lambda_4^{N-n}-2\lambda_2^{N-n-1})\bar{\mu}_1 s_2^{n+1}x_1^{n+1}}{(k_s+s_2^{n+1})(k_p+p^{n+1})^2} - \lambda_5^{N-n}\dfrac{\bar{\mu}_2 k_2 x_2^{n+1}}{(k_2+p^{n+1})^2}\right)}{1+dt\left(D+\dfrac{\bar{\mu}_1 s_2^{n+1}x_1^{n+1}}{(k_s+s_2^{n+1})(k_p+p^{n+1})^2}+\dfrac{\bar{\mu}_2 k_2 x_2^{n+1}}{(k_2+p^{n+1})^2}\right)}, & \\
\lambda_4^{N-n-1} \leftarrow \dfrac{\lambda_4^{N-n} - dt\left(\dfrac{(2\lambda_2^{N-n-1}-\lambda_3^{N-n-1})\bar{\mu}_1 s_2^{n+1}}{(k_s+s_2^{n+1})(k_p+p^{n+1})} + \dfrac{D\bar{\mu}_1 s_2^{n+1}}{(k_s+s_2^{n+1})(k_p+p^{n+1})}\right)}{1+dt\left(\dfrac{\bar{\mu}_1 s_2^{n+1}}{(k_s+s_2^{n+1})(k_p+p^{n+1})}-D\right)}, & \\
\lambda_5^{N-n-1} \leftarrow \dfrac{\lambda_5^{N-n} - dt\dfrac{\lambda_3^{N-n-1}\bar{\mu}_2 p^{n+1}}{k_2+p^{n+1}}}{1-dt\left(\dfrac{\bar{\mu}_2 p^{n+1}}{k_2+p^{n+1}}-D\right)}, & \\
u^{n+1} \leftarrow \max\left(\min\left(\dfrac{\bar{h}}{\beta}\dfrac{\bar{g}s_1^{n+1}}{k_3+s_1^{n+1}}(\lambda_1^{N-n-1}-\lambda_2^{N-n-1}), u^{\max}\right), u^{\min}\right). &
\end{array}
\right.
$$

end